13TH CANADIAN MASONRY SYMPOSIUM
HALIFAX, CANADA
JUNE 4TH – JUNE 7TH 2017

ANALYTICAL MODELLING OF THE OUT-OF-PLANE BEHAVIOUR OF CFRP AND DUCTILE ADHESIVE REINFORCED CLAY BRICK MASONRY WALLS

Wijte, S.N.M.[1]; Türkmen, Ö.S.[2]; Vermeltfoort, A.T.[3] and Martens, D.R.W.[4]

ABSTRACT

In an experimental testing program three different ductile adhesive reinforced masonry configurations were involved. The first configuration consisted of a carbon fibre reinforced polymer (CFRP) strip placed in the heart of the masonry wallettes with a visco-elastic epoxy. The second configuration had an additional surface treatment based on a polymer. The third configuration was similar to the second one, however with a cement based surface treatment with imbedded CFRP net. The results of the experimental tests confirmed the strong increase in both the moment- and flexural capacity and supported the previously stated significant gain in ductility. The purpose of the research was to model out of plane behaviour of QSRM. A discrete model is described that can be used to determine the structural behaviour of non-load bearing clay brick masonry walls which are enhanced by applying the aforementioned reinforcement configurations. The model consists of stiff masonry blocks and discrete joints at the locations of the first cracks. The relation between the internal moment and the rotation in the discrete joint is based on the bond behaviour of the CFRP strips and, when it is applied, the polymer finish. The bonding behaviour of the CFRP strips is derived from pull-out tests. The results of the model are compared with results from experimental research after the out of plane behaviour of clay brick masonry walls has been enhanced with the ductile adhesive configurations. From this comparison it is concluded that the model is able to describe the experimental out of plane behaviour.

KEYWORDS: *CFRP, modelling, out-of-plane, seismic, retrofit*

[1] Full Professor, Department of the Built Environment, Section Structural Design, Eindhoven University of Technology, P,O, Box 513, 5600 MB, Eindhoven, S.N.M.Wijte@tue.nl
[2] PhD Candidate, Department of the Built Environment, Section Structural Design, Eindhoven University of Technology, P,O, Box 513, 5600 MB, Eindhoven, O.S.Turkmen@tue.nl
[3] Associate Professor, Department of the Built Environment, Section Structural Design, Eindhoven University of Technology, P,O, Box 513, 5600 MB, Eindhoven, A.T.Vermeltfoort@bwk.tue.nl
[4] Full Professor, Department of the Built Environment, Section Structural Design, Eindhoven University of Technology, P,O, Box 513, 5600 MB, Eindhoven, D.R.W.Martens@tue.nl

INTRODUCTION

In Groningen, an area in the North-East of the Netherlands, earthquakes occur as a result of the subsidence of the ground at relatively shallow depth beneath the earth's surface. This subsidence is caused by the extraction of gas from the Groningen gasfield. These so-called "induced" earthquakes are distinguished from the common and well known "tectonic" earthquakes, which occur as a result of ground movements in the deep crust. Another distinctive aspect is that the soft claylike soil in Groningen transmits the vibrations than does a rocky soil. Research and measurements done by KNMI provides a contour plot of peak ground acceleration in Groningen [1]. The maximum value in this contour plot is 0.36g with a return period of 475 years.

The majority of buildings in Groningen is composed of unreinforced single leaf masonry designed for relatively moderate wind loads. Therefore it is essential to improve the earthquake resistance of the current buildings in the area to prevent building collapse, with likely casualties. Due to the slenderness of the load bearing walls, the lateral load bearing capacity is mostly critical.

Some key aspects need to be taken into account when selecting a suitable solution. Ductility is one of the most important requirements for all kinds of seismic resistant structures. Unreinforced masonry, which lacks ductility, often fails in a brittle manner. When it is shaken severely it cracks and falls apart in a number of pieces. Therefore it is essential to "tie it together". Prior research concluded that the existing materials used in stand-alone retrofit systems were insufficient and needed improvement [2]. By applying a specially developed glue and combining two stand-alone seismic retrofit measures, an amplifying effect in terms of load bearing capacity and ductility was reached. The proposed patented seismic retrofit system, QuakeShield, was tested in bending on wallettes. Due to the rather small scale of the initial research, one of the conclusions pointed to the necessity of a broader experimental program in order to gain more knowledge.

An extensive experimental research program was conducted to investigate the behaviour of Carbon Fiber Reinforced Polymer (CFRP) and ductile adhesive reinforced masonry [3]. Using these experimental results, this paper will focus on developing an analytical model of the out of plane behaviour of CFRP and ductile adhesive reinforced clay brick masonry walls.

CONFIGURATIONS

In total five configurations were considered for modelling: QSS+, QSS-, QSC+, QSC- and QSP+. The strengthening process started by milling deep (65 mm) grooves of 15 mm in width with a 325 mm center-to-center distance on half-brick wallettes of 1250 x 650 mm, CFRP strips (20x1.4 mm) were imbedded in the grooves using a specially developed visco-elastic adhesive: QuakeShield Epoxy (QSE). These deeply placed CFRP strips strengthened the wallettes for out-of-plane (OOP) loading in both directions, whilst only treating one side of the surface. After the strips were placed, one of the two types of surface treatment could be applied if applicable: 1 - PolyUrea based (QSP), or 2 - Cement based with imbedded CFRP net (QSC). The configuration without surface finishing is coded as QSS. The plus sign after the specimen code indicates that the treated surface was subjected to tension due to bending, whereas the minus sign indicates the same for the non-treated

surface. Based on the results of the experimental program [2], mean load-displacement multi-linear curves were constructed and used for further analysis. This is provided in Figure 1 and Table 1.

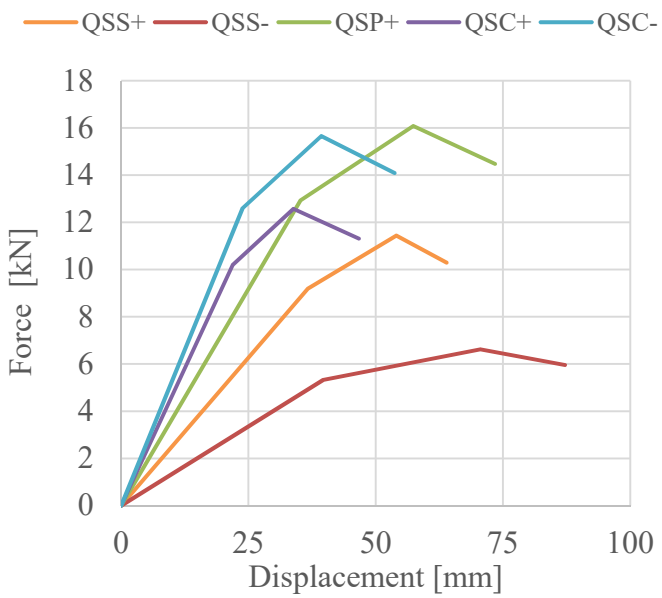

Figure 1: Mean force-displacement diagram of the 5 configurations

Table 1: Mean force-displacement of the 5 configurations

Specimen		Displ. (mm)	Force [kN]
QSS+	80%	36,71	36,71
	100%	54,08	54,08
	90%*	63,92	63,92
QSS-	80%	39,69	39,69
	100%	70,56	70,56
	90%*	87,18	87,18
QSP+	80%	35,24	12,93
	100%	57,41	16,09
	90%*	73,47	14,48
QSC+	80%	21,92	10,19
	100%	33,84	12,57
	90%*	46,72	11,31
QSC-	80%	23,85	12,60
	100%	39,34	15,66
	90%*	53,72	14,09

* Post-peak

PULL-OUT BEHAVIOR

In order to model the behaviour, the results of previously conducted pull-out test were also analyzed. 6 specimens were cut out from larger clay brick masonry wallettes. The dimensions of the smaller specimens were 240 mm (height) x 220 mm (width) x 100 mm (thickness). In each specimen a groove of 15 mm in width and 20 mm in depth was milled. After priming the groove, the QuakeShield Epoxy and CFRP strips were installed, with three different anchorage lengths as shown in Table 2. The CFRP strips extended 250 mm above the specimen. This is done to provide enough space for the clamp. A schematic view of the specimen with full anchorage length is provided in Figure 2. Four LVDT's measured the loaded end slip of the CFRP strip with respect to the top surface of the specimen. The tests were performed on CFRP strips with different dimensions than the strips that are standard applied in the system. The test set-up is shown in Figure 3. The properties of the strips used in the pull-out tests versus the standard strips are provided in Table 3.

Table 2: Specimens pull-out tests

Specimen	Anchor length (mm)
OH1, OH2	±230
OH3, OH4	±175
OH5, OH6	±115

Table 3: Material properties CFRP strips

Parameter	Unit	Pull-out	Standard
Width	mm	15	20
Thickness	mm	2,5	1,4
Tensile capacity	kN	≥105	≥78,5
Modulus of elasticity	kN/mm^2	≥170	≥205
Elongation at break	%	>16	13,5

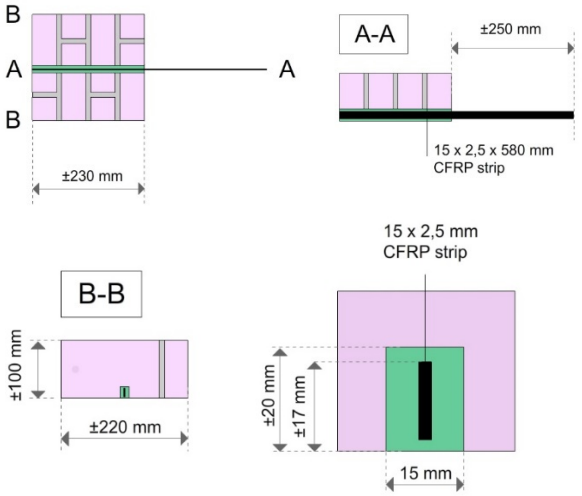

Figure 2: Schematic overview of the specimen with full anchorage length

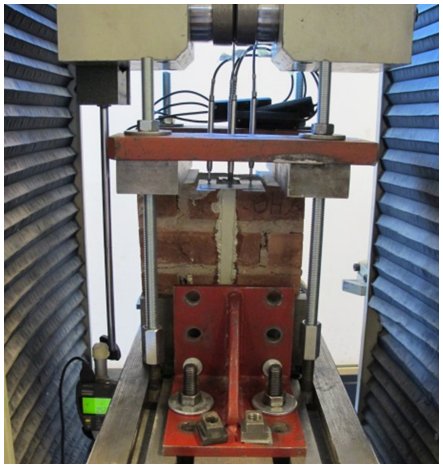

Figure 3: Pull-test setup

The results of the pull-out tests are provided in Table 4 and Figure 4. The energy provided in Table 3.1 is the area under the force-displacement diagram. The displacement is based on the average value of the four LVDT sensors. Linear regression of the test data showed that the pull-out force (kN) equals 50 times the embedded length (m).

Table 4: Results of the pull-out tests

Specimen code	OH1	OH2	OH3	OH4	OH5	OH6
Anchor length [m]	0.230	0.230	0.175	0.175	0.115	0.115
Pull-out force [kN]	11.38	12.36	8.81	7.87	5.84	6.03
Energy	31.38	35.84	22.01	22.18	18.45	13.90

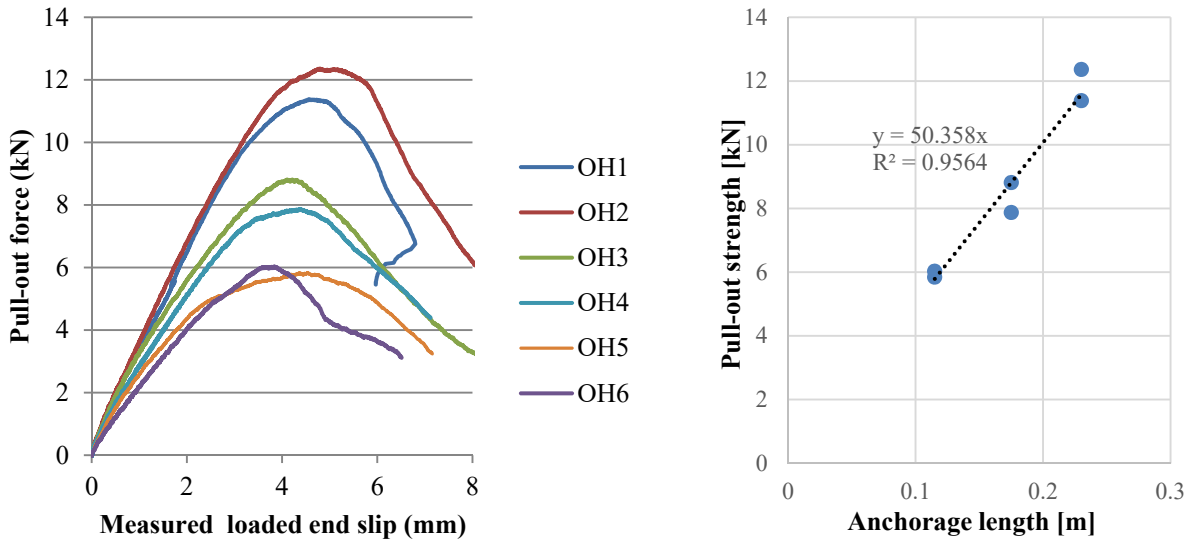

Figure 4: Results of the pull-out tests: force-displacement graphs and correlation between the pull-out strength and the embedded length

MODEL FOR BOND-SLIP BEHAVIOUR OF QSS

The bond-slip behaviour of the combination of a CFRP-strip and QuakeShield Epoxy is derived from the pull-out tests. The tests clearly showed that the bond behaviour is mainly determined by the properties of the QuakeShield Epoxy. A linear distribution of the shear force between the CFRP-strip and the masonry is assumed. The maximum pull-out force depends on the embedded length l_{em} [mm]:

$$F_s[\mathrm{kN}] = K_Q \cdot l_{em} = 50 \cdot \frac{l_{em}}{1000} \tag{1}$$

The relationship between the force in the strip and the slip is obtained by fitting a multilinear function to the experimentally retrieved data. The relationship between the slip between the strip and the surrounding masonry (Δ_s) and the shear force (q_s) is described by the following expressions:

$$q_s[\tfrac{kN}{mm}] = 15\left[\tfrac{kN}{mm^2}\right] \cdot \Delta_s[mm] \qquad \text{for } \Delta_s \leq 3\ mm \tag{2}$$

$$q_s = 45\ [\tfrac{kN}{mm}] + 5\left[\tfrac{kN}{mm^2}\right](\Delta_s - 3mm) \qquad \text{for } 3\ mm < \Delta_s \leq 4\ mm \tag{3}$$

$$q_s = 50\ [\tfrac{kN}{mm}] + 5{,}7\left[\tfrac{kN}{mm^2}\right](\Delta_s - 4mm) \qquad \text{for } 4\ mm < \Delta_s \leq 7\ mm \tag{4}$$

$$q_s = 0 \qquad \text{for } \Delta_s > 7\ mm \tag{5}$$

The force in the strip then follows from:

$$F_s[kN] = q_s\left[\tfrac{kN}{mm}\right] \cdot l_{em}[mm] \tag{6}$$

MODEL FOR OUT-OF-PLANE BEHAVIOUR OF QSS

The bond behaviour of the CFRP-strips and the bending behaviour of the QSS specimens is such that it is chosen to neglect other deformations and to describe the out-of-plane behaviour of the specimens in a discrete way as shown in Figure . It is assumed that during the test, the specimen consists of three stiff masonry blocks and that the deformation of the specimen is the result of the deformation in the joints between the three blocks.

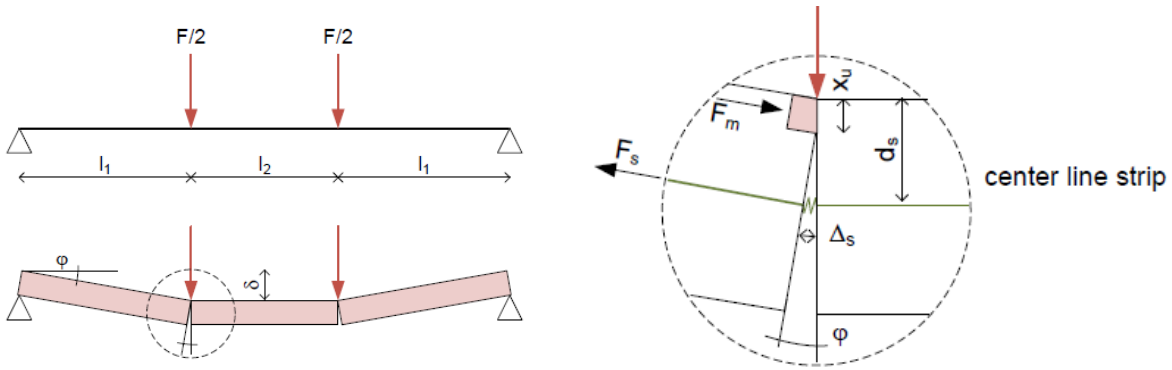

Figure 5: Model for describing the out-of-plane behaviour of QSS specimens

The internal moment in the joint is the result of the compression force in the compression zone of the stiff masonry block, the tension force in the CFRP-strip (which is represented by a linear spring) and the lever arm between these forces. The distance between the centre line of the strip and the edge of the masonry on the compression side is considered to be the effective depth of the cross section (d_s). It is assumed that the lever arm (z_s) equals the effective depth minus one-half of the assumed depth of the compression zone (x_u):

$$z_s[mm] = d_s[mm] - \frac{x_u[mm]}{2} \tag{7}$$

The internal moment is the result of the product of the force in the strip, the lever arm and the number of strips present (n_s):

$$M_{int}[kN \cdot mm] = n_s \cdot F_s[kN] \cdot z_s[mm] \tag{8}$$

The rotation in the joint (φ) can be obtained by:

$$\varphi[-] = \frac{\Delta_s[mm]}{d_s[mm] - x_u[mm]} \tag{9}$$

The relation between the rotation in the joint and the displacement at midspan of the specimen follows from:

$$\delta[mm] = \varphi \cdot l_1[mm] \tag{10}$$

For equilibrium, the internal moment in the joint should equal the external moment in the joint:

$$F[kN] = \frac{2M_{int}[kN \cdot mm]}{l_1[mm]} \tag{11}$$

From these equations, for a given displacement at midspan, the relation with the external load (F) can be found:

$$\varphi = \frac{\delta[mm]}{l_1[mm]} \tag{11}$$

$$\Delta_s[mm] = \varphi(d[mm] - x_u[mm]) \tag{12}$$

where Δ_s is the slip of the strip in the end block. Due to the fact that the force in the strip in the mid-block is constant, no slip will occur in this block. From Δ_s the value for q_s and F_s can be derived from equations 2-6. From this the external moment can be found:

$$F = \frac{2M_{int}[kN \cdot mm]}{l_1\,[mm]} = \frac{2 \cdot n_s \cdot F_s[kN] \cdot z_s[mm]}{l_1[mm]} \tag{13}$$

Figure shows a comparison between the model and the test data. The figure clearly shows that the chosen model results is a good description of the structural behaviour of the QSS-specimens.

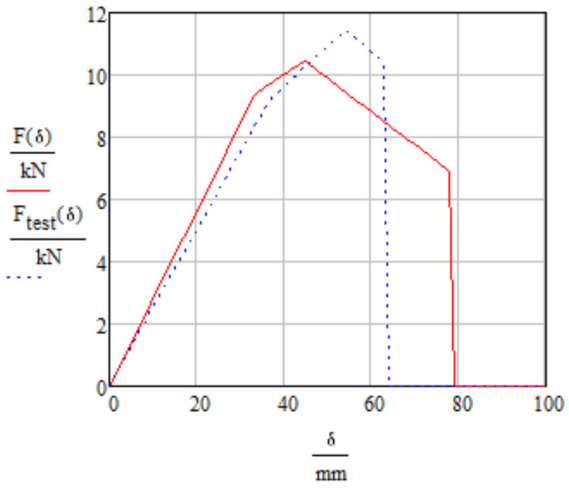

Figure 6: Comparison between the force-displacement graph of the experiments and model for QSS specimens

MODEL FOR OUT-OF-PLANE BEHAVIOUR OF QSP

The QSP-specimen consists of a centered CFRP-strip and a polymer-based finish, which both have a tensile capacity. Depending on the direction of the load the polymer finish can be either on the compression (QSP-) or tension side (QSP+) of the specimen. The structural behaviour of the QSP-specimens is identical to the QSS specimens. Due to the significant difference in Young's modulus between the masonry and the polymer finish, the polymer finish will not make a significant contribution in withstanding the compression force in the cross-section. The out-of-plane behaviour of QSP- specimens can therefore be described by the same model used for the QSS specimens.

However, the test results clearly showed a positive contribution of a polymer finish applied on the tension side of the specimen (QSP+). The previous model for describing the QSS specimens is therefore adjusted. The discrete model is extended with an additional spring that describes the structural properties of the polymer based finish as shown in Figure .

The polymer finish is applied on the surface of the masonry and is therefore not completely straight and flat. The stiffness of the spring can therefore not be derived directly from the mechanical properties of the polymer. It is assumed that the spring behaves linear until a certain elongation (Δ_p) and that after that point the force in the finish reduces. Based on fitting to the results of the external force displacement relation of the QSP+ specimens the following relation between the force and deformation is used for the specimens with a width of 650 mm:

$$F_p\left[\frac{kN}{mm}\right] = 1.3\left[\frac{kN}{mm^2}\right] \cdot \Delta_p[mm] \qquad \text{for } \Delta_p \leq 12\ mm \qquad (14)$$

$$F_p = 23.4\ \left[\frac{N}{mm}\right] + 0.65\ \left[\frac{kN}{mm^2}\right] \Delta_p[mm] \qquad \text{for } 12\ mm < \Delta_p \leq 17\ mm \qquad (15)$$

$$F_p = 0 \qquad \text{for } \Delta_p > 14\ mm \qquad (16)$$

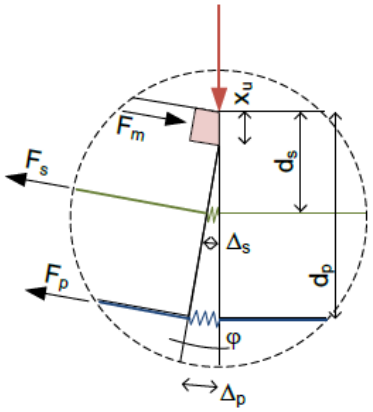

Figure 7: Model for describing the out-of-plane behaviour of QSP+ specimens

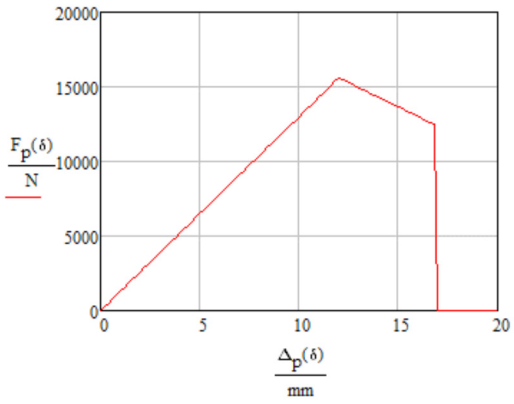

Figure 8: Relation between the force and the slip in the polymer finish

From 7 the relationship between the deformation of the CFRP-strip (Δ_s) and the polymer finish (Δ_p) can be derived:

$$\Delta_p[mm] = \Delta_s[mm]\,\frac{d_p[mm] - x_u[mm]}{d_s[mm] - x_u[mm]} \qquad (17)$$

The moment in the joint follows from:

$$M_{int}[kN \cdot mm] = n_s \cdot F_s[kN] \cdot z_s[mm] + F_p[kN] \cdot z_p[mm] \qquad (18)$$

Where z_s is calculated according to equation 7. The lever arm of the polymer layer (z_p) equals the effective depth minus one-half of the assumed depth of the compression zone (x_u):

$$z_p[mm] = d_p[mm] - \frac{x_u[mm]}{2} \qquad (19)$$

The rotation in the joint follows from equation 9. The elongation of the polymer layer can be determined using:

$$\Delta_p[mm] = \varphi(d_p[mm] - x_u[mm]) \tag{20}$$

From Δ_s the value for q_s and F_s can be derived from equations 2-6.. From Δ_p the force in the polymer finish F_p can be derived as previously described in equations 14-16. From the equilibrium M_{int} equals M_{ext} the external force F can be found:

$$F[kN] = \frac{2M[kN \cdot mm]}{l_1[mm]} = \frac{2}{l_1[mm]}\left(n_s \cdot F_s[kN] \cdot z_s[mm] + F_p[kN] \cdot z_p[mm]\right) \tag{21}$$

Comparison between the model and the test results (see Figure) shows that the described model results in a good description of the structural behaviour of the QSP+ specimens.

MODEL FOR OUT-OF-PLANE BEHAVIOUR OF QSC

The QSC-specimen consists of a centered CFRP-strip and a cementitious-based finish with an embedded CFRP-net, which both have a tensile capacity. Depending on the direction of the load the finish can either be on the compression (QSC-) or tension side (QSC+) of the specimen.

In the QSC- configuration the cement matrix layer, which has a greater compressive strength than masonry, is on the compression side of the specimen. Therefor it is assumed that the internal compression force, which results from the moment, is resisted by the cement matric and the effective depth of the CFRP-strip is increased by 15 mm. This also means a reduction in the depth of the compressive zone. Besides these minor adjustments the same model is applied for the QSC-specimens as for the QSS specimens. Figure shows a comparison between the experi-mental data and the model for the QSC- specimens. Apart from this figure we can conclude that the chosen model results in a good description of the structural behaviour of the QSC- specimens.

Due to the tensile capacity of the cement matrix CFRP-net the resistance against external loading is greater that for the QSS specimens. The force-displacement graphs of the QSC+ speci-mens showed a drop in resistance after a first large peak [2]. The load increases again for a second path to a lower peak. The test results showed that the CFRP-net is not able to resist the tensile force in the cement layer when it cracks. Therefore it is concluded that the QSC+ specimens behave like the QSS specimens after the first peak. Although the cement finish will increase the stiffness of the specimen this will not influence the assumed model consisting of rigid blocks and joints.

In the QSC+ experiments the cement matrix was present between the masonry and the support. Due to this a tensile force was raised in the cement matrix that lead to cracks which introduced flexure shear failure of the specimens. To prevent this for the QSC+ specimens, the set-up was changed to a three point bending test. Therefore a three point bending test was conducted on QSC+ specimens. The model should be adjusted slightly, see Figure 11.

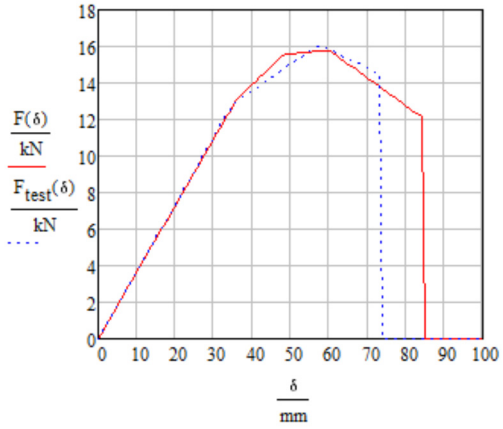

Figure 9: Comparison between the force-displacement graph of the experiments and model for QSP+ specimens

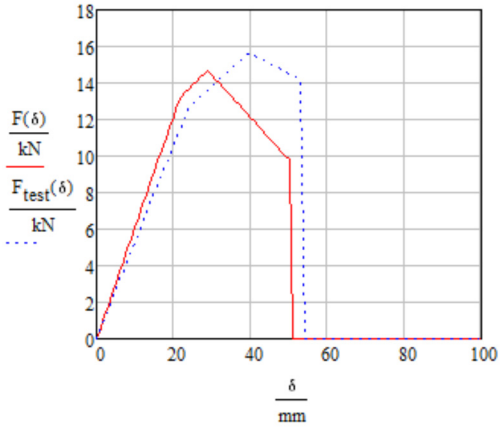

Figure 10: Comparison between the force-displacement graph of the experiments and model for QSC- specimens

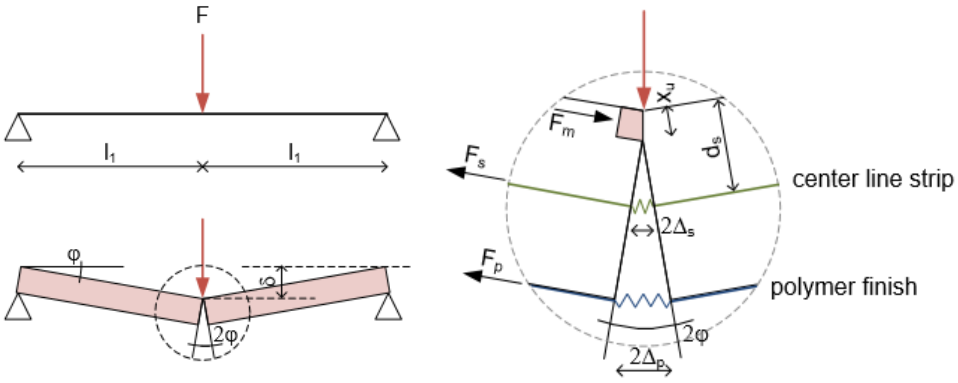

Figure 11: Model for describing the out-of-plane behaviour of QSC+ specimens in a three point bending test

Equations 7-13 are used to describe the out-of-plane behaviour of QSC+ specimens. The comparison in Figure 1 shows good agreement between the model and the experiments.

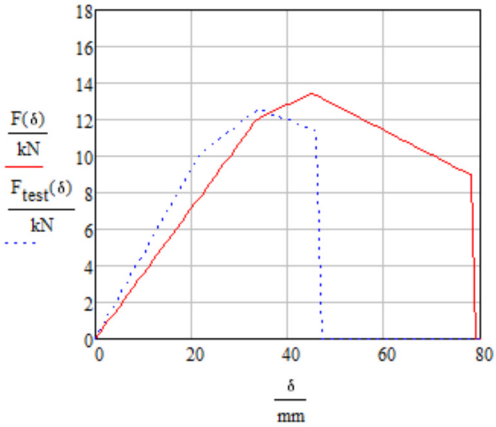

Figure 1: Comparison between the force-displacement graph of the experiments and model for QSC+ specimens

CONCLUSION

In this paper a straightforward model for describing the out-of-plane behaviour of CFRP and ductile adhesive reinforced masonry has been presented. The model consists of stiff masonry blocks connected by discrete joints at the locations of the maximum moment. The relation between the internal moment and the rotation in the joint is based on the bond behaviour of the CFRP-strips and, if applied, the polymer finish. The tensile capacity of the cement matrix and the CFRP-net is not taken into account. It was found that the models are able to describe the structural behaviour of QuakeShield-reinforced masonry panels quite well.

RECOMMENDATIONS

The following recommendations are made in order to get more insight on the bond slip behaviour:

- Direct and beam pull-tests to gain more knowledge on the bond-slip behaviour of CFRP strips imbedded in the visco-elastic epoxy.
- Check if the assumed linear distribution of the shear force between the CFRP-strip and the masonry is valid.

Finally, another aspect that should be taken into account is the introduction of cyclic loading to investigate degradation effects. This is especially important for cyclic earthquake loads.

ACKNOWLEDGEMENTS

The authors wish to thank and acknowledge Royal Oosterhof Holman and SealteQ for supporting this research into the behavior of a new seismic retrofit system.

REFERENCES

[1] NPR 9998 (2015). “Assessment of structural safety etc., seismic loads induced earthquakes” (In Dutch: “Beoordeling van de constructieve veiligheid van een gebouw bij nieuwbouw, verbouw en afkeuren - Grondslagen voor aardbevingsbelastingen: Geïnduceerde aard-bevingen”), *NEN*, Delft, Netherlands.

[2] Türkmen, Ö.S., Vermeltfoort, A.T. and Martens, D.R.W. (2016). “Seismic retrofit system for single leaf masonry buildings in Groningen.” *Proc., 16th International Brick and Block Masonry Conference*, Padova, Italy, on USB.

[3] Türkmen, Ö.S. , Vermeltfoort, A.T. , Wijte, S.N.M. , Martens, D.R.W. (2017). “Experiments to determine the out of plane behaviour of CFRP and ductile adhesive reinforced clay brick masonry walls.” *Proc., 13th Canadian Masonry Symposium*, Halifax, Nova Scotia, Canada.